



Contents lists available at ScienceDirect

# Colloids and Surfaces A: Physicochemical and Engineering Aspects

journal homepage: [www.elsevier.com/locate/colsurfa](http://www.elsevier.com/locate/colsurfa)

## Mannosyl, glucosyl or galactosyl liposomes to improve resveratrol efficacy against Methicillin Resistant *Staphylococcus aureus* biofilm

Stefano Aiello<sup>a,b,1</sup>, Livia Pagano<sup>a,b,1</sup>, Francesca Ceccacci<sup>b</sup>, Beatrice Simonis<sup>a,b</sup>,  
 Simona Sennato<sup>c</sup>, Francesca Bugli<sup>d,e,\*\*</sup>, Cecilia Martini<sup>e</sup>, Riccardo Torelli<sup>d,e</sup>,  
 Maurizio Sanguinetti<sup>d,e</sup>, Alessia Ciogli<sup>f</sup>, Cecilia Bombelli<sup>b,\*</sup>, Giovanna Mancini<sup>g</sup>

<sup>a</sup> Sapienza University, Department of Chemistry, P.le A. Moro 5, Rome, Italy

<sup>b</sup> CNR-Institute for Biological Systems (ISB) Secondary Office of Rome-Reaction Mechanisms c/o Department of Chemistry, Sapienza University, P.le A. Moro 5, Rome, Italy

<sup>c</sup> CNR-Institute of Complex Systems (ISC)- Sede Sapienza c/o Physics Department, Sapienza University, P.le A. Moro 5, Rome, Italy

<sup>d</sup> Dipartimento di Scienze di Laboratorio e Infettivologiche, Fondazione Policlinico Universitario "A. Gemelli" IRCCS, 00168, Rome, Italy

<sup>e</sup> Dipartimento di Scienze Biotecnologiche di Base, Cliniche Intensivologiche e Perioperatorie, Università Cattolica del Sacro Cuore, Rome, Italy

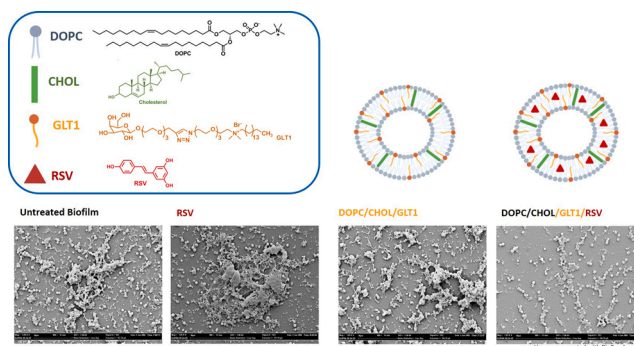
<sup>f</sup> Sapienza University, Department of Chemistry and Technology of Drug, P.le A. Moro 5, Rome, Italy

<sup>g</sup> CNR- Institute for Biological Systems (ISB), Area della Ricerca di Roma 1, Via Salaria Km 29,300, 00015 Monterotondo, Italy

### HIGHLIGHTS

- Resveratrol glycoliposomes for Methicillin Resistant *Staphylococcus aureus* biofilm.
- Galactosyl-amphiphile targets Methicillin Resistant *Staphylococcus aureus* biofilm.
- Cationic galactosyl-amphiphiles enhance liposomes binding to biofilm.
- Cationic galactosylated liposomes enhance resveratrol delivery to biofilm.

### GRAPHICAL ABSTRACT



\* Corresponding author at: CNR-Institute for Biological Systems (ISB) secondary office of Rome-Reaction Mechanisms c/o Department of Chemistry, Sapienza University, P.le A. Moro 5, 00185 Rome Italy.

\*\* Corresponding author at: Dipartimento di Scienze di Laboratorio e Infettivologiche, Fondazione Policlinico Universitario "A. Gemelli" IRCCS, and Dipartimento di Scienze Biotecnologiche di Base, Cliniche Intensivologiche e Perioperatorie, Università Cattolica del Revised Manuscript [Unmarked Text] Sacro Cuore, Largo Agostino Gemelli 8, 00168 Rome, Italy.

E-mail addresses: [stefano.aiello@uniroma1.it](mailto:stefano.aiello@uniroma1.it) (S. Aiello), [livia.pagano@uniroma1.it](mailto:livia.pagano@uniroma1.it) (L. Pagano), [francesca.ceccacci@cnr.it](mailto:francesca.ceccacci@cnr.it) (F. Ceccacci), [beatrice.simonis@uniroma1.it](mailto:beatrice.simonis@uniroma1.it) (B. Simonis), [simona.sennato@roma1.infn.it](mailto:simona.sennato@roma1.infn.it) (S. Sennato), [francesca.bugli@unicatt.it](mailto:francesca.bugli@unicatt.it) (F. Bugli), [ceciliamartini84@gmail.com](mailto:ceciliamartini84@gmail.com) (C. Martini), [riccardo.torelli@policlinicogemelli.it](mailto:riccardo.torelli@policlinicogemelli.it) (R. Torelli), [maurizio.sanguinetti@unicatt.it](mailto:maurizio.sanguinetti@unicatt.it) (M. Sanguinetti), [alessia.ciogli@uniroma1.it](mailto:alessia.ciogli@uniroma1.it) (A. Ciogli), [cecilia.bombelli@cnr.it](mailto:cecilia.bombelli@cnr.it) (C. Bombelli), [giovanna.mancini@cnr.it](mailto:giovanna.mancini@cnr.it) (G. Mancini).

<sup>1</sup> These authors contributed equally.

<https://doi.org/10.1016/j.colsurfa.2021.126321>

Received 22 December 2020; Received in revised form 7 February 2021; Accepted 9 February 2021

Available online 18 February 2021

0927-7757/© 2021 Elsevier B.V. All rights reserved.

## ARTICLE INFO

## Keywords:

Cationic liposomes  
Glycoliposomes  
Galactosylamphiphile  
Mannosylamphiphile  
Glucosylamphiphile  
Trans-resveratrol  
MRSA biofilm

## ABSTRACT

Novel cationic glycoliposomes, composed of 1,2-dioleoyl-*sn*-glycero-3-phosphocholine (DOPC), cholesterol (Chol) and glycoamphiphiles featuring a galactosyl, mannosyl or glucosyl moiety have been investigated for the targeted delivery of *trans*-resveratrol (RSV), a Quorum Sensing Inhibitor (QSI), to *Methicillin Resistant Staphylococcus Aureus* (MRSA) biofilms.

All the glycosylated formulations show a 10–20 % reduction of their hydrodynamic size and a high positive increase in  $\zeta$ -potential (20÷27mV), with respect to the almost neutral DOPC/Chol liposomes (-3.7 mV). RSV is entrapped in liposomes with high Entrapment Efficiency (EE%), the formulations containing glycosylated amphiphiles showing higher values of EE% (79–90 %) than those containing DOPC/CHOL (65 %). In all the liposomal formulations, the inclusion of RSV causes a decrease in  $\zeta$ -potential, which is particularly evident in the negative value of DOPC/Chol liposomes (-14.8 mV). This is probably due to the ionization of a small percentage of RSV molecules that point towards the lipid/water interface, as reported in the literature.

Greater antioxidant activity is found when RSV is embedded in glycosylated liposomes, rather than DOPC/CHOL liposomes. This finding suggests a different RSV distribution in the lipid membrane enclosing the glycosylated amphiphiles, which favor an external exposure of RSV.

Biological assays carried out to monitor the demolition effect of RSV-loaded liposomes on mature biofilm of MRSA show that the presence of cationic glycoamphiphiles is essential for a demolition effect to take place on the biofilm matrix. In particular, RSV-galactosylated liposomes are the most effective in destroying MRSA biofilm even at a RSV concentration (0.019 mM) sixty times lower than the MIC (1.2 mM). This work demonstrates, for the first time, how the functionalization of liposomes with cationic glycosidic residues can enhance liposome performances as QSI nanocarriers for the treatment of biofilm associated infections.

## 1. Introduction

Biofilm-enhanced infections have become one of the biggest threats to human health and a serious challenge for modern medicine. Every year, biofilm associated infections are responsible for hundreds of thousands of chronic infections all over the world and, according to many studies, 60 %–80 % of all bacterial infections and almost all nosocomial infections involve biofilms [1,2].

An exhaustive definition of biofilm has been proposed by Donlan and Costerton: “A microbially derived sessile community characterized by cells that are irreversibly attached to a substratum or interface or to each other; are embedded in a matrix of extracellular polymeric substances that they have produced and exhibit an altered phenotype with respect to growth rate and gene transcription” [3]. This community is “a spatially heterogeneous structure” [4], constantly varying in form, in which growth and metabolic rate, oxygen and nutrient availability, cell density, size and morphology differ markedly within the biofilm structure [4].

All higher organisms, including humans, are colonized by millions of microorganisms forming biofilms. Biofilms are also responsible for contamination of process water, deterioration of the hygienic quality of drinking water and microbially influenced corrosion [5].

Biofilms are associated with high levels of resistance to antimicrobials, frequent failures of treatment, increased morbidity and mortality.

Usually, antibiotic treatment destroys only the detached planktonic bacteria, leaving the biofilm intact. In this way, bacterial biofilms act as nests for acute infections that regularly come back after some weeks or months of incubation. It has been shown that, while dormant, cells in biofilms become increasingly resistant to antimicrobial agents. Vancomycin, for example, is decreasingly efficient in killing aging biofilm after 6 h, 24 h and 48 h [6].

In the last decade, some methods for treating biofilm-enhanced infections have been developed, but the problem is still far from being solved. Many of the several approaches that have been proposed to fight these infections, such as the development of new anti-adhesive materials or the use of ultrasonication and magnetic fields to eradicate biofilm or achieve drug penetration, while promising for the inhibition of biofilm formation on environmental and clinical abiotic surfaces, do not solve the problem of infections in humans [7].

A promising approach for fighting biofilm-associated bacterial

infections involves the use of *Quorum Sensing Inhibitors* (QSI), small molecules that have inhibitory capacities against *Quorum Sensing* (QS), a system of communication among cells inside the biofilm [8].

Recently it has been reported that resveratrol (RSV) can inhibit the process of QS. Indeed, RSV is able to inhibit the biofilm growth of both Gram-positive and Gram-negative bacteria [9–11]. In particular, biological tests on *Staphylococcus aureus*, *Bacillus cereus*, *Staphylococcus epidermidis* have shown that RSV is able to inhibit the process of QS among bacterial cells by blocking their initial adhesion to the surface [12]. Experiments on *Helicobacter pylori* cultures have also demonstrated that very low concentrations of resveratrol can inhibit the growth and even kill bacterial cells [13].

While this wide spectrum of antimicrobial activity, coupled with its safety profile (it has been granted Generally Recognised As Safe, GRAS, status) [14] and relatively low price, makes RSV very attractive for the development of new pharmaceutical products, several problems have emerged such as those related to RSV’s low solubility in water, low bioavailability and instability in biological fluids.

Nevertheless, the development of an appropriate drug delivery system based on liposomes could solve most of these issues. Indeed, the inclusion of RSV inside liposomes enhances its water solubility and stability [7,15], and could make it a successful strategy against some bacterial infections. In fact, RSV-loaded liposomes are able to exert stronger anti-oxidative and anti-inflammatory activities than free RSV [16], inhibit biofilm formation and promote biofilm dispersion even at sub-MIC concentrations, displaying anti-QS activity [17].

Here we describe the preparation and characterization of novel liposome formulations for the delivery of *trans*-RSV to *methicillin resistant Staphylococcus aureus* (MRSA) biofilm. The liposome formulations investigated were composed of a natural phospholipid, (1,2-dioleoyl-*sn*-glycero-3-phosphocholine, DOPC), cholesterol (Chol), and a glycosylated amphiphile (either **GL4**, [18,19], **MAN1** or **GLT1**, Chart 1). The glycosylated amphiphiles were devised in order to couple a quaternary ammonium group to a glycosylated moiety and obtain a molecule able to promote both an efficient electrostatic interaction with biofilm and a specific liposome binding to carbohydrate-specific adhesins (*i.e.* lectins) overexpressed on both bacteria cells and biofilm [20].

Our goal was to highlight the ability of glycosylated amphiphiles to enhance liposome binding and, consequently, resveratrol delivery to bacteria biofilm, and to identify the best sugar moiety to target MRSA

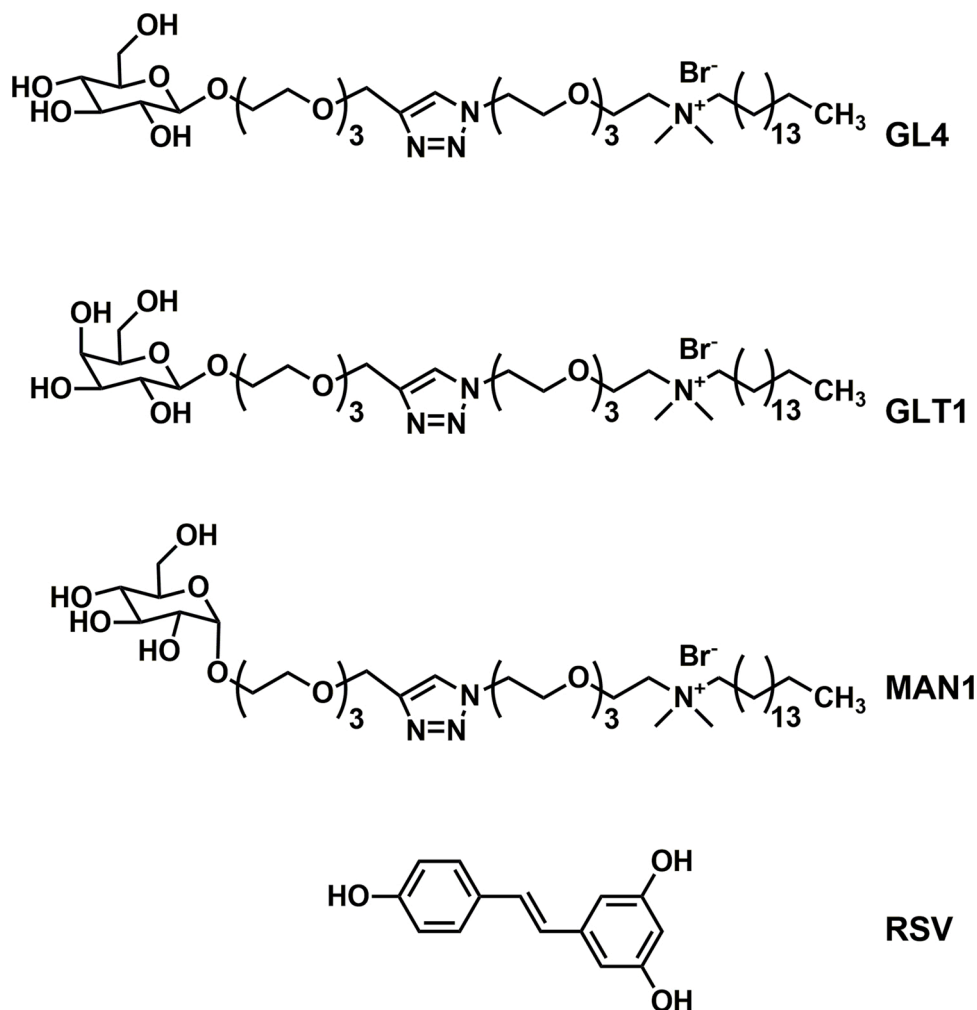


**Chart 1.** Molecular structures of the glycosylated amphiphiles (GL4, GLT1 and MAN1) and RSV.

biofilm.

The anti-biofilm activity of RSV enclosed in the lipid bilayer of liposome formulations was compared with that of free RSV and empty liposomes on MRSA biofilm. In particular, the experiments monitored the demolition effect of liposome formulations on preformed biofilm of the selected organism.

## 2. Experimental section

### 2.1. Materials

DOPC was purchased from Avanti Polar Lipids (Alabaster, AL, USA), phosphate-buffered saline (PBS; 0.01 M phosphate buffer; 0.0027 M KCl);

**Table 1**

Characterization of liposome formulations, both empty and RSV-loaded, tested on MRSA biofilm.

Formulation <sup>a</sup>	Lipid ratio	D <sub>h</sub> <sup>d</sup> (nm)	PDI <sup>d</sup>	ζ-Potential <sup>b,d</sup> (mV)	EE (%)	RSV <sup>d,e</sup> (mM)
<b>LPs and GLPs</b>						
DOPC/Chol	80:20	105 ± 0.7	0.1 ± 0.02	-3.7 ± 0.7	-	-
DOPC/Chol/GL4	75:20:5	81 ± 1.4	0.1 ± 0.01	25.5 ± 2.0	-	-
DOPC/Chol/MAN1	75:20:5	89 ± 0.25	0.2 ± 0.01	27.0 ± 0.6	-	-
DOPC/Chol/GLT1	75:20:5	88 ± 3.3	0.1 ± 0.01	24.4 ± 0.6	-	-
<b>RSV-LPs<sup>c</sup> and RSV GLPs<sup>c</sup></b>						
DOPC/Chol	80:20	106 ± 1	0.2 ± 0.01	-14.8 ± 1.2 (-15.0 ± 2.0)	65	1.17 ± 0.01 (1.81 ± 0.03)
DOPC/Chol/GL4	75:20:5	91 ± 2	0.2 ± 0.01	19.5 ± 1.8 (29.8 ± 1.8)	89	2.27 ± 0.04 (2.56 ± 0.02)
DOPC/Chol/MAN1	75:20:5	101 ± 6	0.2 ± 0.01	26.2 ± 1.6 (25.6 ± 1.1)	79	2.08 ± 0.04 (2.31 ± 0.03)
DOPC/Chol/GLT1	75:20:5	98 ± 3	0.2 ± 0.02	27.1 ± 3.3 (29.2 ± 1.2)	90	2.03 ± 0.043 (2.56 ± 0.02)

<sup>a</sup> Total lipid concentration in all formulations correspond to 20 mM.

<sup>b</sup> ζ-Potential values post and before dialysis (data in brackets).

<sup>c</sup> RSV/lipids ratio at the beginning of the preparation is 1:8.

<sup>d</sup> Error associated to D<sub>h</sub>, PDI, ζ-Potential and RSV concentration values is the standard deviation of three repeated measurements on three different samples.

<sup>e</sup> RSV concentration post and before dialysis (data in brackets), both assessed by HPLC.

0.137 M NaCl; pH 7.4), Sephadex G-50 fine, sodium sulphate, *trans*-resveratrol (RSV, purity = 99 %), ABTS (2,2'-azino-bis-[3-ethylbenzothiazoline-6-sulfonate], purity >99 %), *trans*-stilbene (purity = 96 %), cholesterol (purity = 99 %), cellulose dialysis membrane (D9652-100FT, m.w. cut off = 14,000 Da) were purchased from Sigma-Aldrich. Dialysis membrane was activated by washing the tubing under running water for 3–4 h, treating the tubing with a 0.3 % (w/v) solution of sodium sulfide at 80 °C for 1 min, washing with hot water (60 °C) for 2 min, followed by acidification with a 0.2 % (v/v) solution of sulfuric acid, finally rinsing with hot water to remove the acid.

The glycosylated amphiphile **GL4** was previously synthesized by some of us [18]; the synthesis and characterization of the new glycosylated amphiphiles **MAN1** and **GLT1** is reported in the Supporting Information.

## 2.2. Instrumentation

For the extrusion protocol, 10 mL Lipex Biomembranes extruder was used, equipped with Whatman Nuclepore polycarbonate membranes (pore size 0.1 µm).

Sonics Vibra Cell sonicator was used in the preparation procedure of RSV formulations.

PES sterile syringe filters (0.22 µm) for liposomes filtration were purchased from Euroclone.

A Malvern Nano-ZetaSizer apparatus, equipped with a 5 mW HeNe laser ( $\lambda = 632.8$  nm), was used to perform DLS and electrophoretic mobility measurements.

A Cary 300 UV-vis double beam spectrophotometer (Varian Australia PTY Ltd., Mulgrave, Vic., Australia), equipped with a thermostating apparatus for temperature control, was used to carry out OD and UV measurements on liposome suspensions.

A microtiter plate reader (Bio-Rad Laboratories, Hercules, CA) was used to perform the CV assay.

Waters Alliance 2695 (Waters Associates, Milford, MA, USA) coupled with a photodiode array detector (PDA Waters 996) was used to perform HPLC analysis. Data were collected and analyzed using Empower 2 software (Waters, Milford, MA, USA). Scanning Electron Microscopy (SEM) images were obtained using a SEM Supra 25 (Zeiss, Germany).

## 2.3. Preparation of empty and RSV- loaded liposomes

Aqueous dispersions of empty liposomes were prepared according to a reported procedure [21] (Table 1). Lipid films were prepared on the inside wall of a round-bottom flask by evaporation of solutions containing the proper amount of lipid components dissolved in CHCl<sub>3</sub> (DOPC and Chol) or in MeOH (**GL4**, **MAN1** and **GLT1**) to obtain a mixture with the desired molar percentage. Lipid films were kept overnight under reduced pressure (0.4 mbar) and then a proper amount of PBS (one tablet dissolved in 200 mL of deionized water yields 0.01 M phosphate buffer, 0.0027 M potassium chloride and 0.137 M sodium chloride, pH 7.4, at 25 °C) was added to have a lipid dispersion at 20 mM concentration. The aqueous suspensions were vortex-mixed in order to detach the film completely from the flask, then the resulting multilamellar vesicles (MLVs) were freeze-thawed six times from liquid nitrogen to 50 °C and extruded (10 times) through a 100 nm polycarbonate membrane.

For the preparation of RSV loaded liposomes, RSV was added to the lipid mixture in the organic solution before film formation (RSV/lipids molar ratio being 1/8). The procedure for liposome preparation was the same as followed for unloaded liposomes, the only difference being that samples containing RSV were sonicated at 40 W (10 cycles of 10 s) before freezing-thaw cycles in order to break RSV aggregates that usually form in aqueous solutions and thus improve the entrapment inside the lipid bilayer [22].

The removal of untrapped RSV was performed by dialysis in PBS: portions of 500 µL of RSV-liposomes were loaded into 2 mL eppendorfs

that were closed with activated dialysis membrane (1962.5 mm<sup>2</sup>), and fastened with rubber bands. All the eppendorfs were placed in a glass crystallizer containing PBS (25-times the total volume of the sample), with the dialysis membrane in contact with the buffer. The diffusate buffer was changed every 30 min over 2.5 h (four times), and gently stirred throughout. The set up and timing of dialysis were chosen on the basis of preliminary experiments in which the complete depletion of free RSV from the retentate solution (RSV 1.25 mM in PBS/absolute ethanol) was monitored over time. During all steps of the preparation (film formation, extrusion and dialysis), samples were protected from light.

## 2.4. Characterization of liposomes

### 2.4.1. Size and $\zeta$ potential measurements by DLS

Suspensions of liposomes (1 mM total lipids) in 150 mM PBS were analyzed by DLS measurements soon after preparation, after 48 h and after 7 days, to determine the average diameter, the polydispersity index, and the stability over time with respect to fusion.

For the determination of  $\zeta$  potential, liposomes (1 mM total lipids) were suspended in 10 mM PBS and low voltages were applied to avoid the risk of Joule heating effects.

The normalized intensity autocorrelation functions were measured at an angle of 173° and analyzed by using the cumulant method [23]. The first cumulant was used to obtain the apparent diffusion coefficients  $D$  of the particles, further converted into apparent hydrodynamic diameters,  $D_h$ , by using the Stokes–Einstein relationship  $D_h = k_B T / 3\pi\eta D$ , where  $k_B T$  is the thermal energy and  $\eta$  is the solvent viscosity.

Analysis of the Doppler shift to determine the electrophoretic mobility was done by using phase analysis light scattering (PALS) [24], a method which is especially useful at high ionic strengths, where mobilities are usually low. The mobility  $\mu$  of the liposomes was converted into a  $\zeta$ -potential using the Smoluchowski relation  $\zeta = \mu \eta / \epsilon$  where  $\epsilon$  and  $\eta$  are the permittivity and the viscosity of the solution, respectively.

### 2.4.2. Determination of liposomes RSV entrapment efficiency

The content of RSV loaded in liposomes was assessed by HPLC measurement (Table 1). *Trans*-stilbene (TSB) was used as internal standard (concentration  $1 \times 10^{-4}$  M). A calibration curve ( $R^2 = 0.9980$ ) with free RSV samples in the  $8.1 \times 10^{-5}$  -  $8.1 \times 10^{-4}$  M range and TSB at  $1 \times 10^{-4}$  M was built.

Liposomal samples were diluted 1:2 prior injection with a methanol solution containing TSB at a concentration set to have a final TSB concentration of  $1 \times 10^{-4}$  M. Dilution in methanol was needed to break all aggregates.

The HPLC column employed was a C18-SunFire 150  $\times$  4.6 mm ID, 3.5 µm (dp). The mobile phases were water/acetonitrile 95/5 + 0.1 % TFA (solvent A) and methanol + 0.1 % TFA (solvent B). Elution gradient started with A/B 80/20, v/v, in 7 min reached 100 % B (curve 6) and was maintained at 100 %B for 20 min.

All solvents were filtered through 0.45 µm filters before use. The analysis was carried out at 30 °C with a 1 mL/min flow. Triplicate injections were made for each sample and the average area, at 306 nm, was employed to determine RSV concentration.

The entrapment efficiency (EE%) was then calculated using the following equation:

$$EE (\%) = \frac{[RSV]_{pd}}{[RSV]_0} \times 100 \quad (1)$$

where  $[RSV]_{pd}$  indicates RSV concentration after dialysis and  $[RSV]_0$  is the concentration soon after extrusion.

### 2.4.3. Evaluation of anti-oxidant properties of RSV-loaded liposomes (ABTS assay)

In order to assess the antioxidant power of RSV-loaded liposomes, the Total Antioxidative Capacity (TAC) of a sample (from Ozcan Erel



[25–27]) was evaluated. The assay was based on the formation of the radical cation 2,2'-azinobis-[3-ethylbenzothiazoline-6-sulfonate] (ABTS+●, with a characteristic petrol green colour) through oxidation of the neutral, colourless 2,2'-azinobis-[3-ethylbenzothiazolin-6-sulfonic] acid (ABTS) by hydrogen peroxide.

The following reagents were prepared:

- REAGENT 1: Acetate buffer 0.40 M at pH 5.8 was prepared by mixing 235 mL of a 0.40 M CH<sub>3</sub>COONa water solution and 15 mL of a 0.40 M CH<sub>3</sub>COOH water solution.
- REAGENT 2: Acetate buffer 30 mM at pH 3.6 was prepared by mixing 20 mL of a 30 mM CH<sub>3</sub>COONa water solution and 250 mL of a 30 mM CH<sub>3</sub>COOH water solution.
- REAGENT 3: 69 μL of 35 % v/v H<sub>2</sub>O<sub>2</sub> were diluted to 250 mL with Reagent 2. Then 0.27 g of ABTS were diluted in 50 mL of this solution to obtain Reagent 3.

A calibration curve was built following the steps described below.

400 μL of Reagent 1, 10 μL of free RSV samples (RSV 0–0.75 mM in absolute ethanol) and 40 μL of Reagent 3 were mixed in a quartz cuvette (1 cm, 500 μL internal volume) and, starting immediately after mixing, the absorbance at 666 nm was recorded for 20 min. The difference between the curve of ABTS+● and each curve of ABTS+● in the presence of RSV became constant after 5 min, suggesting that after this time the changes in absorbance are not due to the action of RSV but rather to the medium. For this reason, the calibration curve was built using the absorbance at 5 min.

The liposomal formulations were then analyzed as follows: 400 μL of Reagent 1, 10 μL of a liposomal sample (diluted to have RSV concentration 0.25 mM) and 40 μL of Reagent 3 were mixed in a 1 cm quartz cuvette and the absorbance at 666 nm was recorded, starting immediately after mixing, for 5 min.

## 2.5. Bacterial strains and in vitro biofilm formation

The antibiofilm activity of liposomes was determined on mature biofilm of a clinical isolate of *methicillin-resistant Staphylococcus aureus* (MRSA). The isolate was retrieved from the frozen glycerol stocks and streaked on a fresh Trypticase Soy agar 5% sheep blood plate (bio-Merieux), incubated at 37 °C for 18 h and sub cultured to have fresh colonies. MRSA was grown in brain heart infusion (BHI) medium supplemented with 0.25 % glucose, at  $1 \times 10^7$  cfu/mL, and submerged biofilms were established in flat-bottom 96-well microtiter plate wells for 96 h at 37 °C and 5% CO<sub>2</sub>.

## 2.6. Crystal Violet assay

The biofilm formation on multi wells was measured by Crystal Violet (CV) assay. In brief, wells were washed with PBS to remove non-attached bacteria and stained with 100 μL of 0.1 % CV solution. After 45 min at room temperature, plates were emptied and extensively washed with distilled water to remove the excess CV. For biofilm quantification, 50 μL of 95 % ethanol were added to the wells to solubilize all biofilm-associated dye and the absorbance at 630 nm was determined by a microplate reader.

## 2.7. Demolition assay on MRSA biofilm

To test biofilm demolition, the dialyzed suspensions of RSV-loaded liposomes (shown in Table 1) were sterilized through a 0.22 μm PES filter, and diluted with PBS to have a final concentration of 1.2 mM RSV. MRSA biofilms were left to grow for 4 days as described previously. Plates were then incubated at 37 °C overnight. On the fifth day, wells were emptied, washed with PBS and liposomes at RSV concentrations ranging from 1.2 mM to 0.019 mM were added. The plates were then left at 37 °C overnight. Wells were then washed again with PBS before 100 μL

of 0.1 % CV solution were added. After 45 min at room temperature, plates were emptied and washed with distilled water to remove excess CV. For biofilm quantification, 50 μL of 95 % ethanol were added to the wells to solubilize all biofilm-associated dye and the absorbance at 630 nm was determined by a microplate reader.

## 2.8. Scanning electron microscopy (SEM) evaluation

Bacterial biofilms grown on a glass disk and treated with different liposome formulations were investigated by SEM. Fixed and dried biofilms were mounted onto an aluminum stub using double-sided carbon tape and coated with a gold/palladium film (80:20) by using a high-resolution sputter coater (Agar Scientific B7234).

## 2.9. Statistical analysis

All statistical analysis was performed with the support of GraphPad prism version 5.0 and Stata software. Data were analyzed by a one-way ANOVA and post hoc Dunnett' comparison tests ( $p < 0.05$ ).

Results of size and ζ potential represent the average value and the corresponding standard deviation of three different and independent preparations of each liposomal formulation. DLS and -ζ potential measurements were repeated three times on each sample, with each single measurement containing at least 15 different sub-runs, the number of repetitions being optimized by the instrument in order to increase the signal/noise ratio of the measured signal.

## 3. Results and discussion

Glycosylated liposomes, either empty (GLPs) or loaded with RSV (RSV-GLPs), were formulated with a natural unsaturated phospholipid (DOPC), cholesterol (Chol) and a glycosylated amphiphile (GL4, or one of the two newly synthesized amphiphiles, MAN1 and GLT1, Chart 1). Non-glycosylated liposomes (LPs and RSV-LPs) were also prepared for comparison, employing only DOPC and Chol. Cholesterol was added to the lipid mixture to make the lipid bilayer more stable and allow for a large amount of glycosylated amphiphiles to be added to it; in fact, in the absence of cholesterol, these glycosylated lipids have detergent properties when added in large amounts to lipid mixtures, thus yielding micellar aggregates rather than liposomes [18,28].

Liposomes were prepared by the extrusion method, coupled with the freeze-thaw protocol; samples containing RSV were submitted to additional sonication cycles before freeze-thaw, in order to break the RSV aggregates that usually form in aqueous solutions and improve the entrapment in the lipid bilayer [22,24]. Free RSV was removed by dialysis.

Mean diameter, polydispersity index (PDI), ζ-potential, RSV Entrapment Efficiency (EE%) and amount of entrapped RSV of all liposomal formulations are reported in Table 1.

### 3.1. Characterization of liposomes

#### 3.1.1. Size, ζ potential and RSV localization of liposomes

Liposomes size and polydispersity index were evaluated by DLS measurements soon after preparation, and then monitored over time; all formulations were stable up to 7 days. Results of DLS analyses show a narrow monomodal distribution for all LP and GLP formulations prepared in the absence of RSV, with a diameter in agreement with that imposed by the extrusion protocol (100 nm). However, all the glycosylated formulations display a hydrodynamic diameter 10–20 % smaller than DOPC/Chol liposomes. This behavior can be explained on the basis of previous studies carried out by some members of the team on liposomes formulated with GL4, which make it possible to put forward some hypotheses on the arrangement of GL4 within the DOPC/Chol bilayer [29,30].

Molecular dynamics simulation previously performed on DMPC/GL4

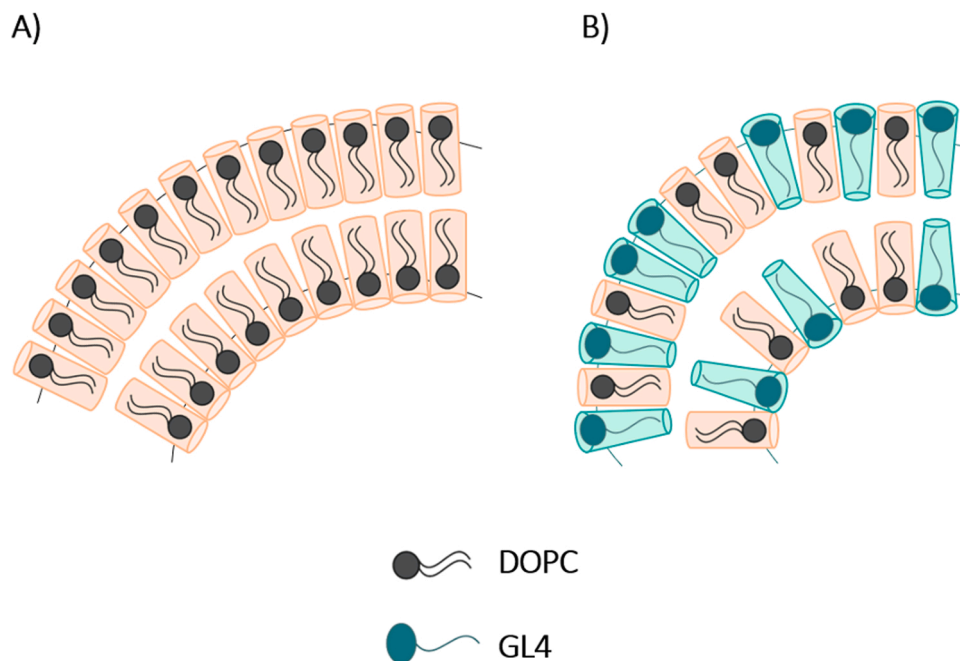


**Fig. 1.** A pictorial representation of A) DOPC bilayer B) DOPC /GL4 mixed bilayer, where GL4 molecular geometry forces the aggregate to adopt a stronger curvature.

bilayers suggested a preferential localization of both the glucose and quaternary ammonium residues at the lipid/water interface, close to the phosphate group, while the triazole ring is embedded deeper in the lipid bilayer, close to the glycerol backbone [18]. Looking at GL4, the structure adopts an overall “L” conformation of the amphiphile, with the hydrophobic chain embedded in the bilayer and the large hydrophilic headgroup extended on the liposome surface [18]. The good exposure of the glucose residue at the lipid/water interfacial region is indirectly confirmed by the fast and efficient agglutination of DMPC/GL4 liposomes in the presence of ConcanavalinA (ConA), a soybean lectin able to bind glucose [28]. Conversely, if GL4 is embedded in DPPC or DOPC liposomes, less agglutination with ConA is observed, suggesting that the sugar residue could be less accessible to the lectin. Therefore, the large headgroup of the amphiphile should be arranged in a different way and the amphiphile as a whole should be embedded deeper in the lipid bilayer of the more hydrophobic DOPC and DPPC phospholipids.

GL4 is characterized by a large headgroup that comprises the sugar, the ammonium group and the hydrophilic spacer. Consequently, it is reasonable to assume that when the amphiphile is embedded in the DOPC/Chol bilayer, the molecule as a whole displays a conical shape, with a larger interfacial area with respect to DOPC, forcing the aggregate to adopt a stronger curvature, thus a smaller diameter (Fig. 1), with respect to DOPC/Chol liposomes. This effect was already reported for other glycosylated liposomes formulated with different natural lipids like EPC [31] or DPPC-PE mixtures [32] and it is more or less similar to what is observed by adding the unsaturated lipid DOPC, characterized by a larger headgroup area per lipid, to DPPC liposomes [33].

Interestingly, the presence of RSV within the lipid bilayer (RSV-GLPs) largely attenuates this effect, which only remains significant in the case of RSV-GLPs formulated with GL4. This evidence is suggestive of the well-known ability of RSV to modulate membrane fluidity and packing [34].

In order to investigate the actual charge of glycosylated liposomes, we measured the  $\zeta$  potential of the 20 mM formulations reported in Table 1. As expected, results show a slightly negative value for DOPC/Chol liposomes, where the presence of RSV further decreases the  $\zeta$  potential. This is in agreement with several studies on RSV localization in biomembrane models reported in the literature. In fact, it has been

shown that, at pH 7.4, in rigid membranes composed of saturated lipids [35,36] or in stiffened membranes composed of EPC:Chol [30], a small percentage of RSV is ionized (~8%) and the negatively charged groups are oriented towards the interface, thus rendering the potential more negative.

The  $\zeta$  potential values of glycosylated liposomes are, on the other hand, positive and quite high. In this case, RSV does not induce significant variations in absolute values. In glycosylated cationic liposomes, RSV is probably located in a deeper region of the membrane, as already observed in other liposomes [24], thus seeming to be less dissociated. Alternatively, RSV's negative charge could be shielded by the highly hydrated headgroup of glycosylated amphiphiles.

The  $\zeta$  potential of RSV-LPs and RSV-GLPs was evaluated soon after extrusion and after the removal of untrapped RSV by dialysis; comparison of the two values is useful for detecting possible depletion of the glycosylated amphiphiles from the lipid bilayer, induced by dialysis. A considerable drop in the  $\zeta$  potential value after dialysis is evident only in the case of liposomes formulated with GL4, suggesting that this amphiphile is partially lost during liposome purification. This is not surprising given that GL4 is more soluble than the other glycosylated amphiphiles and displays a higher *cmc* value ( $4.3 \times 10^{-3}$ M) [26].

### 3.1.2. RSV entrapment efficiency

In order to obtain both high entrapment efficiency and a suitable RSV concentration in the final liposome suspension, we explored different RSV/lipid ratios for the thin film preparation, and concluded that 1:8 is the optimal RSV/lipid ratio for film preparation, as reported by other authors [24]. In fact, higher or lower ratios do not yield an increase in EE %.

Interestingly, the formulations containing glycosylated amphiphiles showed higher EE% values than DOPC/Chol formulations of the same concentration. The greater ability of cationic liposomes to entrap RSV may be due to a favorable association between RSV and quaternary ammonium groups of glycosylated surfactants; this hypothesis is supported by previous works reporting that polyphenols may associate with positively charged tetraalkylammonium moieties [37].

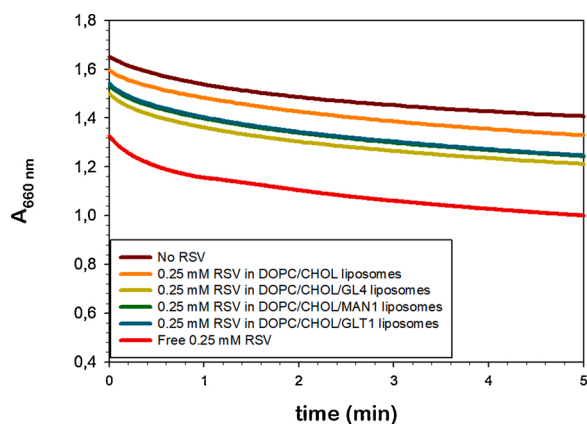


Fig. 2. Absorbance trends of  $ABTS^{+\bullet}$  solutions, alone and in presence of liposomal and free RSV.

### 3.1.3. Evaluation of the anti-oxidant properties of RSV-loaded liposomes

As mentioned in the introduction, RSV has well-known anti-oxidant properties and is, therefore, unstable in the presence of oxidizing agents. In view of this, it is important to assess to what extent the inclusion of RSV in lipid bilayers could protect it from oxidative degradation. The assay used to evaluate the antioxidant capacity of RSV loaded in liposomes was the method reported by Ozcan Erel [26] to assess the Total Antioxidative Capacity (TAC) of a sample. The cation radical ( $ABTS^{+\bullet}$ ), produced by oxidation of ABTS with hydrogen peroxide, is stable at pH 3.6 for up to 6 months [21] at 4 °C, but it decomposes rapidly to its neutral ABTS form at higher pH values. In the presence of reducing agents, the degradation process is faster.

The reduction process of  $ABTS^{+\bullet}$  to ABTS can be followed by UV–vis spectroscopy as the radical cation shows two absorbance bands in the visible region with maxima at 660 nm and 740 nm, respectively, whereas the neutral form does not absorb in this range [21].

To evaluate the protective effect of liposomes on RSV, we followed the absorbance trend of an  $ABTS^{+\bullet}$  solution at 660 nm over time and compared it with the same sample in the presence of either free RSV or liposome-embedded RSV. The  $ABTS^{+\bullet}$  absorbance decay was faster in the presence of free RSV than of liposome-embedded RSV (Fig. 2),

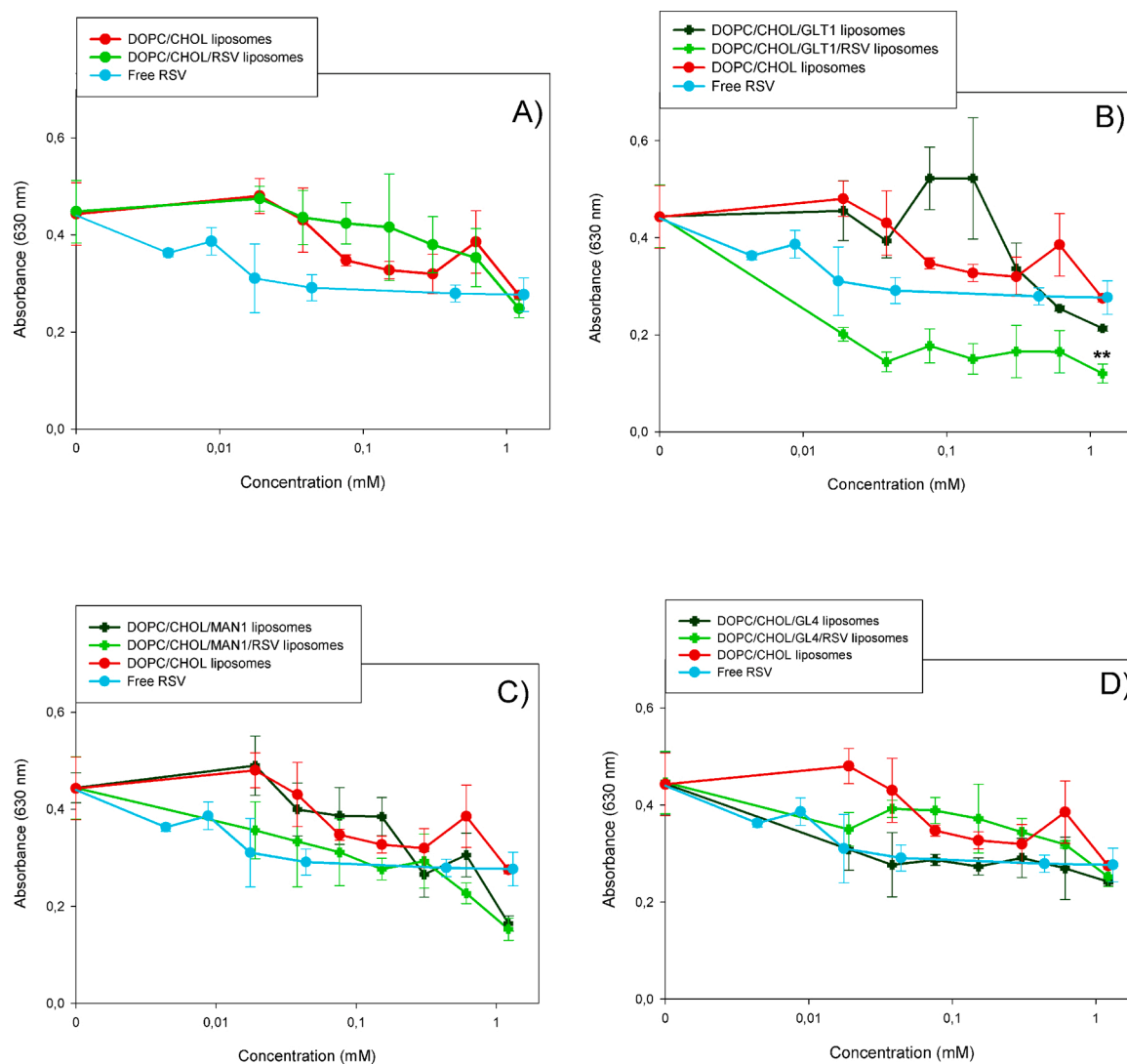


Fig. 3. Biofilm demolition ability of RSV-LPs, RSV-GLPs, LPs, and GLPs, at different RSV concentrations, compared with free RSV. A) DOPC/Chol/RSV and DOPC/Chol compared with free RSV; B) RSV loaded and empty DOPC/Chol/GL4 liposomes compared with free RSV; C) RSV loaded and empty DOPC/Chol/MAN1 liposomes compared with free RSV; D) RSV loaded and empty DOPC/Chol/GLT1 liposomes compared with free RSV. The two asterisks (\*\*) indicate p value smaller than 0.01 ( $p < 0.01$  Dunnett's method multiple comparisons test). In graphs the plot of LPs is reported as blank.



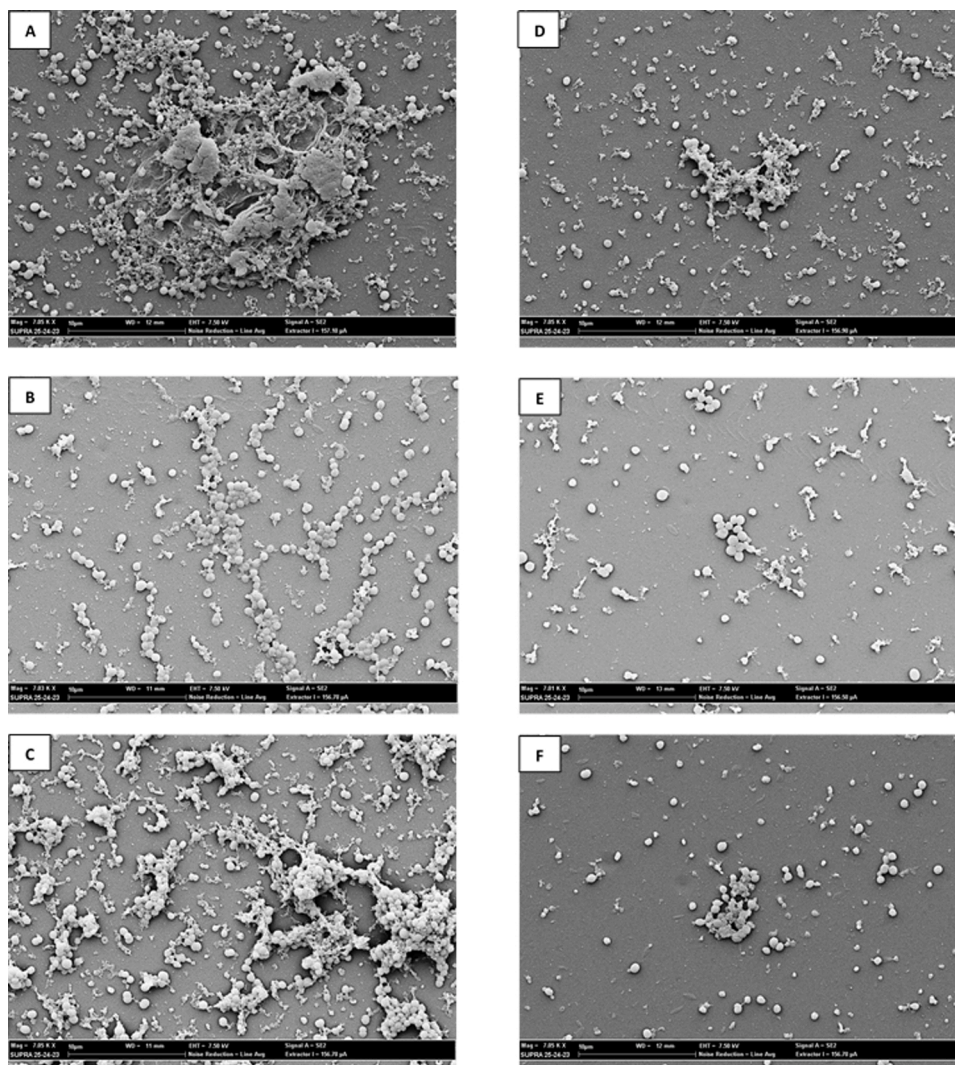


Fig. 4. SEM images of MRSA biofilm treated with A) 0.1 mM free RSV; B) galactosylated RSV-GLPs (RSV 0.1 mM); C) galactosylated GLPs at the same lipidic concentration as B; D) 0.5 mM free RSV; E) galactosylated RSV-GLPs (RSV 0.5 mM); F) galactosylated GLPs at the same lipidic concentration as E.

suggesting that the lipid bilayer provides RSV with some protection. However, the trend observed for samples treated with liposomal RSV formulations indicates a faster  $ABTS^{+\bullet}$  degradation with respect to  $ABTS^{+\bullet}$  in the absence of liposomal RSV, suggesting that the lipid bilayer is not able to shield RSV completely from external agents. This in turn suggests that RSV is partially exposed to the surface and exerts its anti-oxidant activity.

The higher antioxidant efficiency of RSV loaded in glycosylated liposomes with respect to RSV loaded in DOPC/CHOL liposomes supports the hypothesis of a different RSV distribution in the lipid membrane. Thus, the higher  $\zeta$  potential observed in the case of glycosylated liposomes could be correlated to a shielding effect of RSV negative charge by the quaternary ammonium moiety rather than to the deeper insertion of RSV in the lipid bilayer.

### 3.2. Antibiofilm activity evaluation of RSV-GLPs on MRSA

According to the literature about specific lectins and sugar transporters exposed on the external surface of bacteria, the galactosyl moiety should confer liposome specificity towards *Fusobacterium nucleatum* [38] and *Pseudomonas aeruginosa* [39], the glucosyl moiety towards *Helicobacter pylori* [40], *Staphylococcus epidermidis* [19] and *Escherichia coli* [41] and the mannosyl moiety towards *Pseudomonas aeruginosa* [42], *Escherichia coli* [43], *Staphylococcus aureus* [44], and *Enterobacter*

spp. Nevertheless, the ability of galactosyl, glucosyl and mannosyl sugar moieties to recognize and bind with bacterial lectins, once enclosed in amphiphilic molecules with different physico-chemical properties, is not so easy to predict. Therefore, to reveal the efficiency of the above characterized glycosylated liposome formulations in the delivery of RSV to MRSA biofilm, we carried out demolition tests on 4-day-matured MRSA biofilm. The results of the biofilm quantification by CV assay are reported in Fig. 3, where CV absorbance is plotted against RSV concentration. A higher value of absorbance indicates more biofilm materials and, thus, a lower demolition capacity of the formulation. The 0 mM concentration point in each graph is the value obtained by the untreated organisms.

The experimental data demonstrate that non-glycosylated RSV-LPs do not show any demolition ability (Fig. 3, panel A), confirming the importance of both the cationic charge and the glycosylated moieties on the external surface of liposomes for effective delivery of RSV. On the other hand, both mannosylated and galactosylated RSV-GLPs are able to impair the preformed MRSA biofilm, even at very low sub-MIC concentrations (0.019 mM RSV, MIC 1.2 mM), with galactosylated liposomes being the most effective as they are able to demolish the biofilm better than free RSV (Fig. 3, panel D). It is worth noting that empty glycosylated GLPs seem to have more demolition capacity than resveratrol loaded ones. The poor demolition activity of glucosylated RSV-GLPs, could be justified by the drop in  $\zeta$  potential value of GL4-GLPs



after the removal of untrapped RSV by dialysis, suggesting that **GL4** is partially lost during liposome purification. On the contrary, in empty glucosylated liposomes that have not been dialysed, **GL4** may escape from liposomes after interaction with biofilm, giving rise to the formation of micellar aggregates with a highly detergent effect. This probably only occurs for the **GL4** that displays the highest *cmc* value among the three explored amphiphiles.

### 3.3. SEM analysis

The biofilm demolition capacity of galactosylated liposomes was further investigated by means of SEM analysis. After testing free and liposomal RSV at the MIC concentration (1.2 mM) (Fig. S10 Supplementary Material), we analyzed the MRSA biofilm treated with sub-MIC concentrations of free and liposomal RSV. Below are the SEM images of MRSA biofilm treated with two different sub-MIC concentrations of RSV (0.5 and 0.1 mM), both free and loaded into galactosylated liposomes, as well as treated with empty galactosylated liposomes (Fig. 4).

In agreement with the CV assay results, SEM images show that empty galactosylated liposomes have some demolition capacity on the biofilm, which becomes more evident at the higher concentration (Fig. 4 panel G). The RSV-loaded formulation, on the other hand, clearly has a higher demolition capacity than free RSV, even when MIC is diluted tenfold (Fig. 4 panel C).

## 4. Conclusion

In this study, we prepared and characterized three new cationic glucosylated liposome formulations for the delivery of *trans*-resveratrol and investigated their activity in disrupting a mature biofilm of *methicillin resistant Staphylococcus aureus*.

Our results reveal that the three sugar residues have a different biofilm targeting ability on MRSA biofilm. In fact, galactosylated liposomal resveratrol displayed a good demolition capacity against mature MRSA biofilm, even at sub-MIC concentration, while mannosylated RSV liposomes were less efficient and glucosylated liposomal RSV was ineffective.

The entrapment of RSV (or other QSI) in liposomes is known to improve the QSI activity towards biofilm significantly but, to the best of our knowledge, our formulations are the first example of QSI liposomes effectively functionalized for targeting biofilm.

Our findings represent a step forward in the development of efficient nanodrugs able to fight biofilm-associated infections caused by MRSA without inducing resistance.

This novel nanocarrier platform rests on a rational combination of different approaches to fighting bacteria biofilms, involving the use of liposomes, a composition based on cationic lipids or surfactants [45], the delivery of QSI instead of antibiotics [16], and the functionalization for targeting [42,46], all converging in a successful system that had not yet been investigated.

Finally, the potential of all these formulations could be extended to other bacterial strains since the sugar moiety can easily be tuned to assure the optimal liposome-bacterium match for the development of specific delivery systems.

### CRedit authorship contribution statement

**Stefano Aiello:** Investigation, Visualization, Writing - original draft. **Livia Pagano:** Investigation, Funding acquisition, Visualization, Writing - original draft. **Francesca Ceccacci:** Writing - original draft, Validation, Visualization, Writing - review & editing, Funding acquisition. **Beatrice Simonis:** Investigation, Visualization, Writing - review & editing. **Simona Sennato:** Investigation, Formal analysis, Writing - original draft, Writing - review & editing. **Francesca Bugli:** Methodology, Validation, Writing - original draft, Writing - review & editing, Supervision. **Cecilia Martini:** Investigation. **Riccardo Torelli:**

Investigation, Formal analysis, Visualization. **Maurizio Sanguinetti:** Supervision. **Alessia Ciogli:** Methodology, Investigation, Writing - original draft. **Cecilia Bombelli:** Conceptualization, Methodology, Project administration, Funding acquisition, Writing - original draft, Visualization, Writing - review & editing. **Giovanna Mancini:** Conceptualization, Funding acquisition, Supervision.

### Declaration of Competing Interest

The authors report no declarations of interest.

### Acknowledgements

This work was in part supported by CNR-DISBA project “NutrAge” (project nr. 7022) and by PRIN project (call 2018) “BacHounds: Supramolecular nanostructures for bacteria detection” (Prot. 2017E44A9P\_004)

L.P. is grateful to the regional project “Torno Subito” Ed. 2018, funded by POR FSE 2014/2020, for financial support.

### Appendix A. Supplementary data

Supplementary material related to this article can be found, in the online version, at doi:<https://doi.org/10.1016/j.colsurfa.2021.126321>.

## References

- [1] R. Patel, Biofilms and antimicrobial resistance, *Clin. Orthop. Relat. Res.* 437 (2005) 41–47, <https://doi.org/10.1097/01.blo.0000175714.68624.74>.
- [2] H. Flemming, J. Wingender, U. Szewzyk, P. Steinberg, S.A. Rice, S. Kjelleberg, Biofilms: an emergent form of bacterial life, *Nat. Rev. Microbiol.* 14 (2016) 563–575, <https://doi.org/10.1038/nrmicro.2016.94>.
- [3] R.M. Donlan, J.W. Costerton, Biofilm survival mechanism of clinically relevant microorganism, *Clinical Microbiol. Rev.* 15 (2002) 167–193, <https://doi.org/10.1128/CMR.15.2.167-193.2002>.
- [4] G. Laverty, S.P. Gorman, B.F. Gilmore, Biofilm and implant associated infection, in: L. Barnes, I.R. Cooper (Eds.), *Biomaterials and Medical Device - Associated Infections*, Woodhead Publishing, 2015, pp. 18–45.
- [5] K. Forier, K. Raemdonck, S.C. De Smedt, J. Demeester, T. Coenye, K. Braeckmans, Lipid and polymer nanoparticles for drug delivery to bacterial biofilms, *J. Control. Release* 190 (2014) 607–623, <https://doi.org/10.1016/j.jconrel.2014.03.055>.
- [6] M. Monzó, C. Oteiza, J. Leiva, M. Lamata, B. Amorena, Biofilm testing of *Staphylococcus epidermidis* clinical isolates: low performance of vancomycin in relation to other antibiotics, *Diagn. Microbiol. Infect. Dis.* 44 (2002) 319–324, [https://doi.org/10.1016/s0732-8893\(02\)00464-9](https://doi.org/10.1016/s0732-8893(02)00464-9).
- [7] Z. Rukavina, Z. Vanić, Current trends in development of liposomes for targeting bacterial biofilms, *Pharmaceutics* 8 (2016) 18, <https://doi.org/10.3390/pharmaceutics8020018>.
- [8] V.C. Kalia, Quorum sensing inhibitors: an overview, *Biotechnol. Adv.* 31 (2013) 224–245, <https://doi.org/10.1016/j.biotechadv.2012.10.004>.
- [9] S. Gutiérrez, A. Moran, H. Martínez-Blanco, M.A. Ferrero, L.B. Rodríguez-Aparicio, The usefulness of non-toxic plant metabolites in the control of Bacterial Proliferation, *Probiotics Antimicrob. Proteins* 9 (2017) 323–333, <https://doi.org/10.1007/s12602-017-9259-9>.
- [10] I. Kolouchová, O. Mařátková, M. Paldrychová, Z. Kode, E. Kvasničková, K. Sigler, A. Cejková, J. Šmidrkal, K. Demnerová, J. Masák, Resveratrol, pterostilbene, and baicalein: plant-derived anti-biofilm agents, *Folia Microbiol.* 63 (2018) 261–272, <https://doi.org/10.1007/s12223-017-0549-0>.
- [11] M. Man-Ying Chan, Antimicrobial effect of resveratrol on dermatophytes and bacterial pathogens of the skin, *Biochem. Pharmacol.* 63 (2002) 99–104, [https://doi.org/10.1016/s0006-2952\(01\)00886-3](https://doi.org/10.1016/s0006-2952(01)00886-3).
- [12] L. Paulo, S. Ferreira, E. Gallardo, J.A. Queiroz, F. Domingues, Antimicrobial activity and effects of resveratrol on human pathogenic bacteria, *World J. Microbiol. Biotechnol.* 26 (2010) 1533–1538, <https://doi.org/10.1007/s11274-010-0325-7>.
- [13] G.B. Mahady, S.L. Pendland, L.R. Chadwick, Resveratrol and red wine extracts inhibit the growth of CagA+ strains of *Helicobacter pylori* in vitro, *Am. J. Gastroenterol.* 98 (2003) 1440–1441, <https://doi.org/10.1111/j.1572-0241.2003.07513>.
- [14] Determination of generally recognized as safe (GRAS) status of resveratrol as a nutrient supplement, <http://wayback.archiveit.org/7993/20171031055001/https://www.fda.gov/downloads/Food/IngredientsPackagingLabeling/GRAS/NoticeInventory/ucm264051.pdf>, 2007.
- [15] K. Forier, K. Raemdonck, S.C. De Smedt, J. Demeester, T. Coenye, K. Braeckmans, Lipid and polymer nanoparticles for drug delivery to bacterial biofilms, *J. Control. Release* 190 (2014) 607–623, <https://doi.org/10.1016/j.jconrel.2014.03.055>.

- [16] M.W. Jørholm, N. Škalko-Basnet, G. Acharya, P. Basnet, Resveratrol-loaded liposomes for topical treatment of the vaginal, inflammation and infections, *Eur. J. Pharm. Sci.* 79 (2015) 112–121, <https://doi.org/10.1016/j.ejps.2015.09.007>.
- [17] A. Duarte, A.C. Alves, S. Ferreira, F. Silva, F.C. Domingues, Resveratrol inclusion complexes: antibacterial and anti-biofilm activity against *Campylobacter* spp. and *Acrobacter butzleri*, *Food Res. Int.* 77 (2015) 244–250, <https://doi.org/10.1016/j.foodres.2015.05.047>.
- [18] A. Mauceri, S. Borocci, L. Galantini, L. Giansanti, G. Mancini, A. Martino, L. Salvati Manni, C. Sperduto, Recognition of concanavalin A by cationic glucosylated liposomes, *Langmuir* 30 (2014) 11301–11306, <https://doi.org/10.1021/la502946t>.
- [19] I. Francolini, L. Giansanti, A. Piozzi, B. Altieri, A. Mauceri, G. Mancini, Glucosylated liposomes as drug delivery systems of usnic acid to address bacterial infections, *Colloids Surf. B Biointerfaces* 181 (2019) 632–638, <https://doi.org/10.1016/j.colsurfb.2019.05.056>.
- [20] I. Ofek, D.L. Hasty, N. Sharon, Anti-adhesion therapy of bacterial diseases: prospects and problems, *FEMS Immunol. Med. Microbiol.* 38 (2003) 181–191, [https://doi.org/10.1016/S0928-8244\(03\)00228-1](https://doi.org/10.1016/S0928-8244(03)00228-1).
- [21] D.E. Koppel, Analysis of macromolecular polydispersity in intensity correlation spectroscopy: the method of cumulants, *J. Chem. Phys.* 57 (1972) 4814–4820, <https://doi.org/10.1063/1.1678153>.
- [22] W.W. Tschamner, Mobility measurements by phase analysis, *Appl. Opt.* 40 (2001) 3995–4003, <https://doi.org/10.1364/AO.40.003995>.
- [23] M.J. Hope, M.B. Bally, G. Webb, P.R. Cullis, Production of large unilamellar vesicles by a rapid extrusion procedure: characterization of size distribution, trapped volume and ability to maintain a membrane potential, *Biochim. Biophys. Acta* 812 (1985) 55–65, [https://doi.org/10.1016/0005-2736\(85\)90521-8](https://doi.org/10.1016/0005-2736(85)90521-8).
- [24] C. Bonechi, S. Martini, L. Ciani, S. Lamponi, H. Rebmann, C. Rossi, S. Ristori, Using liposomes as carriers for polyphenolic compounds: the case of trans-resveratrol, *PLoS One* 7 (2012) e41438, <https://doi.org/10.1371/journal.pone.0041438>.
- [25] O. Erel, A novel automated direct measurement method for total antioxidant capacity using a new generation, more stable ABTS radical cation, *Clin. Biochem.* 37 (2004) 277–285, <https://doi.org/10.1016/j.clinbiochem.2003.11.015>.
- [26] S. Battista, M.A. Maggi, P. Bellio, L. Galantini, A.A. D'Archivio, G. Celenza, R. Colaiezzi, L. Giansanti, Curcuminoids-loaded liposomes: influence of lipid composition on their physicochemical properties and efficacy as delivery systems, *Colloids Surf. A* 597 (2020), 124759, <https://doi.org/10.1016/j.colsurfa.2020.124759>.
- [27] S. Battista, P. Campitelli, L. Galantini, M. Köberd, G. Vargas-Nadal, L. N. Ventosa, Giansanti, Use of N-oxide and cationic surfactants to enhance antioxidant properties of (+)-usnic acid loaded liposomes, *Colloids Surf. A* 585 (2020) 124154, <https://doi.org/10.1016/j.colsurfa.2019.124154>.
- [28] N. Firon, I. Ofek, N. Sharon, Carbohydrate-binding sites of the mannose-specific fimbrial lectins of enterobacteria, *Infect. Immun.* 43 (1984) 1088–1090, <https://doi.org/10.1128/IAI.43.3.1088-1090.1984>.
- [29] A. Mauceri, A. Fracassi, M. D'Abramo, S. Borocci, L. Giansanti, A. Piozzi, L. Galantini, A. Martino, V. D'Aiuto, G. Mancini, Role of the hydrophilic spacer of glucosylated amphiphiles included in liposome formulations in the recognition of Concanavalin A, *Colloids Surf. B* 136 (2015) 236–239, <https://doi.org/10.1016/j.colsurfb.2015.09.016>.
- [30] D.G. Villalva, L. Giansanti, A. Mauceri, F. Cecacci, G. Mancini, Influence of the state of phase of lipid bilayer on the exposure of glucose residues on the surface of liposomes, *Colloids Surf. B* 159 (2017) 557–563, <https://doi.org/10.1016/j.colsurfb.2017.08.025>.
- [31] L. Latxague, S. Ziane, O. Chassande, A. Patwa, M.J. Dalilaab, P. Barthélémy, Glucosylated nucleoside lipid promotes the liposome internalization in stem cells, *Chem. Commun.* 47 (2011) 12598–12600, <https://doi.org/10.1039/c1cc13948g>.
- [32] T. Miyazawa, R. Kamiyoshihara, N. Shimizu, T. Harigae, Y. Otoki, J. Ito, S. Kato, T. Miyazawa, K. Nakagawa, Amadori-glycated phosphatidylethanolamine enhances the physical stability and selective targeting ability of liposomes, *R. Soc. Open Sci.* 5 (2018), 171249, <https://doi.org/10.1098/rsos.171249>.
- [33] Y. Kurniawan, K.P. Venkataramanan, C. Scholz, G.D. Bothun, n-Butanol partitioning and phase behavior in DPPC/DOPC membranes, *J. Phys. Chem. B* 116 (2012) 5919–5924, <https://doi.org/10.1021/jp301340k>.
- [34] A.R. Neves, C. Nunes, S. Reis, New insights on the biophysical interaction of resveratrol with biomembrane models: relevance for its biological effects, *J. Phys. Chem. B* 119 (2015) 11664–11672, <https://doi.org/10.1021/acs.jpcc.5b05419>.
- [35] Q. Fei, D. Kent, W.M. Botello-Smith, F. Nur, S. Nur, A. Alsamrah, P. Chatterjee, M. Lambros, Y. Luo, Molecular mechanism of resveratrol's lipid membrane protection, *Sci. Rep.* 8 (2018) 1587, <https://doi.org/10.1038/s41598-017-18943-1>.
- [36] A.R. Neves, C. Nunes, H. Amenitsch, S. Reis, Effects of resveratrol on the structure and fluidity of lipid bilayers: a membrane biophysical study, *Soft Matter* 12 (2016) 2118–2126, <https://doi.org/10.1039/c5sm02905h>.
- [37] E.G. Yanes, S.R. Gratz, A.M. Stalcup, Tetraethylammonium tetrafluoroborate: a novel electrolyte with a unique role in the capillary electrophoretic separation of polyphenols found in grape seed extracts, *Analyst* 125 (2000) 1919–1923, <https://doi.org/10.1039/b004530f>.
- [38] P.A. Murray, D.G. Kern, J.R. Winkler, Identification of a galactose-binding lectin on *Fusobacterium nucleatum* FN-2, *Infect. Immun.* 56 (1988) 1314–1319, <https://doi.org/10.1128/IAI.56.5.1314-1319.1988>.
- [39] N. Gilboa-Garber, *Pseudomonas aeruginosa* lectins, *Methods Enzymol.* 83 (1982) 378–385, [https://doi.org/10.1016/0076-6879\(82\)83034-6](https://doi.org/10.1016/0076-6879(82)83034-6).
- [40] P.L. Bardonnnet, V. Faivre, P. Boullanger, M. Ollivon, F. Falson, Glucosylated liposomes against *Helicobacter pylori*: behavior in acidic conditions, *Biochem. Biophys. Res. Commun.* 383 (2009) 48–53, <https://doi.org/10.1016/j.bbrc.2009.03.117>.
- [41] Z. Shu, J. Li, N. Mu, Y. Gao, T. Huang, Y. Zhang, Z. Wang, M. Li, Q. Hao, W. Li, L. He, C. Zhang, W. Zhang, X. Xue, Y. Zhang, Expression, purification and characterization of galectin-1 in *Escherichia coli*, *Protein Expr. Purif.* 99 (2014) 58–63, <https://doi.org/10.1016/j.pep.2014.03.013>.
- [42] D. Passos da Silva, M.L. Matwchuk, D.O. Townsend, C. Reichhardt, D. Lamba, D. J. Wozniak, The *Pseudomonas aeruginosa* lectin LecB binds to the exopolysaccharide Psl and stabilizes the biofilm matrix, *Nat. Commun.* 10 (2019) 10201–10204, <https://doi.org/10.1038/s41467-019-10201-4>.
- [43] L. Öhman, K.E. Magnusson, O. Stendahl, The mannose-specific lectin activity of *Escherichia coli* type 1 fimbriae assayed by agglutination of glycolipid-containing liposomes, erythrocytes, and yeast cells and hydrophobic interaction chromatography, *FEMS Microbiol. Lett.* 14 (1982) 149–153, <https://doi.org/10.1111/j.1574-6968.1982.tb08653>.
- [44] S.P. Vyas, V. Sihorkar, S. Jain, Mannosylated liposomes for bio-film targeting, *Int. J. Pharm.* 330 (2007) 6–13, <https://doi.org/10.1016/j.ijpharm.2006.08.034>.
- [45] C.V. Montefusco-Pereira, B. Formicola, A. Goes, F. Re, C.A. Marrano, F. Mantegazza, C. Carvalho-Wodarz, G. Fuhrmann, E. Caneva, F. Nicotra, C. M. Lehr, L. Russo, Coupling quaternary ammonium surfactants to the surface of liposomes improves both antibacterial efficacy and host cell biocompatibility, *Eur. J. Pharm. Biopharm.* 149 (2020) 12–20, <https://doi.org/10.1016/j.ejpb.2020.01.013>.
- [46] Y. Meng, X. Hou, J. Lei, M. Chen, S. Cong, Y. Zhang, W. Ding, G. Li, X. Li, Multifunctional liposomes enhancing target and antibacterial immunity for antimicrobial and anti-biofilm against methicillin-resistant *Staphylococcus aureus*, *Pharm. Res.* 33 (2016) 763–775, <https://doi.org/10.1007/s11095-015-1825-9>.